

Influence of Quark Boundary Conditions on the Pion Mass in Finite Volume

J. Braun,¹ B. Klein,² and H.J. Pirner^{1,3}

¹*Institute for Theoretical Physics, University of Heidelberg, Philosophenweg 19, 69120 Heidelberg*

²*GSI, Planckstrasse 1, 64159 Darmstadt*

³*Max-Planck-Institut für Kernphysik, Saupfercheckweg 1, 69117 Heidelberg*

(Dated: February 8, 2020)

We calculate the mass shift for the pion in a finite volume with renormalization group (RG) methods in the framework of the quark-mesons model. In particular, we investigate the importance of the quark effects on the pion mass. As in lattice gauge theory, the choice of quark boundary conditions has a noticeable effect on the pion mass shift in small volumes, in addition to the shift due to pion interactions. We compare our results to chiral perturbation theory calculations and find differences due to the fact that chiral perturbation theory only considers pion effects in the finite volume.

I. INTRODUCTION

In the study of QCD, non-perturbative methods are essential in order to understand the connection between the high-momentum regime dominated by quarks and gluons, and the low-momentum regime described in terms of baryonic degrees of freedom. Lattice gauge theory is a method of great importance in this quest. Current simulations with dynamical fermions are limited to quark masses that are rather large compared to the physical values, and to rather small lattice sizes. In addition to taking the continuum limit, in which the lattice spacing is taken to zero, results from lattice calculations require extrapolation towards the chiral limit and the thermodynamic limit. Thus, in order to compare a result for an observable simulated in a small volume with the physical observable, it is essential to understand the finite volume effects.

The most important tool for extrapolations of lattice gauge theory results to small pion masses and to large volumes is chiral perturbation theory (chPT) [1, 2, 3, 4, 5, 6, 7]. In

particular for the chiral extrapolation to small pion masses [1, 8, 9], and for the extrapolation to infinite volume for properties of the nucleon [3], chiral perturbation theory describes the lattice results very well.

In contrast to these applications, the finite volume shifts of the meson masses are less well described by chiral perturbation theory [10, 11, 12]. For the pion mass, the shifts predicted by chiral perturbation theory are consistently smaller than those observed in lattice simulations.

One issue which cannot be addressed by chiral perturbation theory is the influence of the boundary conditions for the quark fields. While fermionic fields require anti-periodic boundary conditions in the Euclidean time direction, we are free to choose either periodic (p. b.c.) or anti-periodic (a.p. b.c.) boundary conditions in the spatial directions. In lattice calculations, this choice changes the finite size effects: In the investigation [13] of finite volume effects it was found that the choice of the boundary conditions for the quark fields has a direct influence on the size of the observed finite volume shifts [13, 14] and can be explained in terms of quark effects. Such effects cannot be captured by a description in terms of pion fields only.

To illustrate this point further, in Fig. 1, we present an example of a lattice calculation in quenched approximation from the ZeRo-collaboration [11]. Shown is the shift of the pion mass $m_\pi(L)$ in finite volume relative to the value in infinite volume $m_\pi(\infty)$ as a function of $m_\pi(\infty) \cdot L$ where L is the volume size. Surprisingly, these results show a dropping pion mass for intermediate volume sizes in a region where the standard chiral perturbation theory result (indicated by the solid lines in the figure) predicts only a very weak volume dependence. This behavior would be unexpected from pion effects alone. In addition, finite volume effects from chiral perturbation theory are predicated on the presence of a “pion cloud”, which in turn requires the presence of sea quarks [3]. Effects for the meson masses similar to those in this quenched calculation are also seen in studies of finite size effects with dynamical quarks [10, 12].

In this paper, we investigate the volume dependence of the pion mass in the quark meson model using renormalization group (RG) methods. In particular, our purpose is to extend our previous work [15] and to investigate the influence of different boundary conditions for the fermionic fields on the finite volume effects for low-energy observables such as the pion mass and the pion decay constant.

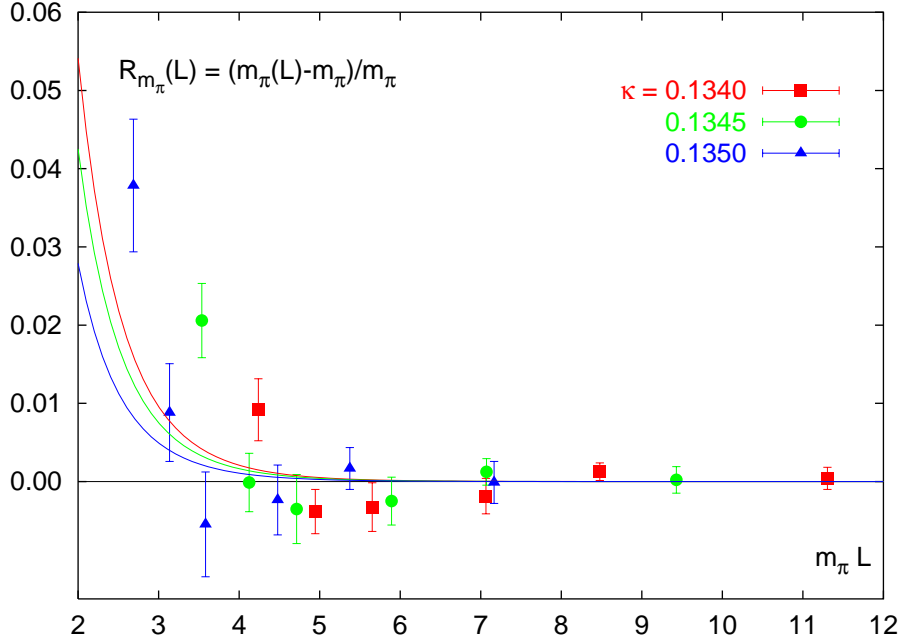


FIG. 1: The pion mass shift $R[m_\pi(L)] = (m_\pi(L) - m_\pi(\infty))/m_\pi(\infty)$ as a function of $m_\pi(\infty) \cdot L$, obtained in a quenched lattice calculation, from ref. [11]. Shown are results for three different values of the quark mass, determined by κ . The solid lines show the corresponding predictions from chiral perturbation theory.

The quark-meson model cannot predict the volume dependence of pion mass and pion decay constant exactly. It is not a gauge theory and thus has neither gluons nor quark confinement. At moderate energies, below the hadronic mass scale, unconfined constituent quarks appear instead of baryonic degrees of freedom. On the other hand, the model has been rather successfully employed in the description of the chiral phase transition [16, 17]. The low-energy couplings of the linear sigma-model with quarks are compatible with those of chiral perturbation theory [18]. As we have previously shown [15], for small pion masses and large volumes our results for the volume dependence agree with those of chiral perturbation theory [4, 5], if we apply anti-periodic boundary conditions for the quark fields in the spatial directions. In this paper, we investigate the effect of different boundary conditions for the quark fields on low-energy observables, namely the pion mass and pion decay constant, in more detail.

In spite of the shortcomings of our model, we believe that the current approach can shed light on lattice results regarding the volume dependence of the pion mass [11, 12, 13]. While

the actual mechanism in QCD may be different due to the presence of color interactions, the approach employed in the present paper gives a possible explanation for the apparent drop in the pseudoscalar pion mass in small volumes observed in [10, 11, 12], which precedes the rise of this mass due to chiral symmetry restoration in extremely small volumes.

The paper is organized as follows: In section II, we briefly introduce the model and the renormalization group equations which govern the RG flow in a finite volume. In section III, we solve the flow equations numerically and in section IV we present the results for the volume dependence of the pion mass. A comparison to lattice results and our conclusions are found in section V.

II. RG-FLOW EQUATIONS FOR THE QUARK-MESON MODEL

As motivated in the introduction, we will use an $O(4)$ -invariant linear σ -model with $N_f^2 = 4$ mesonic degrees of freedom $(\sigma, \vec{\pi})$, coupled to $N_f = 2$ flavors of constituent quarks in an $SU(2)_L \otimes SU(2)_R$ invariant way. This model does not contain gluonic degrees of freedom, and it is not confining, but it is an effective low-energy model for dynamical spontaneous chiral symmetry breaking at intermediate scales of $k \lesssim \Lambda_{UV}$. The ultraviolet scale $\Lambda_{UV} \approx 1.5$ GeV is determined by the validity of a hadronic representation of QCD. At the UV scale Λ_{UV} , the quark-meson-model is defined by the bare effective action

$$\Gamma_{\Lambda_{UV}}[\phi] = \int d^4x \left\{ \bar{q}(\not{\partial} + gm_c)q + g\bar{q}(\sigma + i\vec{\tau} \cdot \vec{\pi}\gamma_5)q + \frac{1}{2}(\partial_\mu\phi)^2 + U_{\Lambda_{UV}}(\phi) \right\} \quad (1)$$

with a current quark mass term gm_c which explicitly breaks the chiral symmetry. The mesonic potential is characterized by two couplings:

$$U_{\Lambda_{UV}}(\phi) = \frac{1}{2}m_{UV}^2\phi^2 + \frac{1}{4}\lambda_{UV}(\phi^2)^2. \quad (2)$$

In a Gaussian approximation, we obtain the one-loop effective action for the scalar fields ϕ ,

$$\Gamma[\phi] = \Gamma_{\Lambda_{UV}}[\phi] - \text{Tr} \log \left(\Gamma_F^{(2)}[\phi] \right) + \frac{1}{2} \text{Tr} \log \left(\Gamma_B^{(2)}[\phi] \right) \quad (3)$$

where $\Gamma_B^{(2)}[\phi]$ and $\Gamma_F^{(2)}[\phi]$ are the inverse two-point functions for the bosonic and fermionic fields, evaluated at the vacuum expectation value of the mesonic field ϕ . We consider the effective action Γ in a local potential approximation (LPA), where the expectation value is taken to be constant over the entire volume. In order to regularize the functional traces,

we use the Schwinger proper time representation of the logarithms. A scale dependence is introduced through an infrared cutoff function

$$k \frac{\partial}{\partial k} f_a(\tau k^2) = -\frac{2}{\Gamma(a+1)} (\tau k^2)^{a+1} e^{-\tau k^2}, \quad (4)$$

which regularizes the Schwinger proper time integral. By replacing the bare coupling in the inverse two-point functions with the scale-dependent running couplings, we obtain a renormalization group flow equation for the effective potential in infinite volume for zero temperature:

$$k \frac{\partial}{\partial k} U_k(\sigma, \vec{\pi}^2, T \rightarrow \infty, L \rightarrow \infty) = \frac{k^{2(a+1)}}{16a(a-1)\pi^2} \left\{ -\frac{4N_c N_f}{(k^2 + M_q^2(\sigma, \vec{\pi}^2))^{a-1}} \right. \\ \left. + \frac{1}{(k^2 + M_\sigma^2(\sigma, \vec{\pi}^2))^{a-1}} + \frac{N_f^2 - 1}{(k^2 + M_\pi^2(\sigma, \vec{\pi}^2))^{a-1}} \right\} \quad (5)$$

In infinite volume, $a = 2$ is the lowest possible integer value we can choose in order to be able to perform the Schwinger-proper time integration. Note that in LPA, the effective action reduces to the effective potential through the relation

$$\Gamma_k[\phi] = \int d^4x U_k(\sigma, \vec{\pi}^2). \quad (6)$$

Due to the fact that we allow for explicit symmetry breaking, the effective potential becomes a function of σ and $\vec{\pi}^2$. The meson masses are the eigenvalues of the second derivative matrix of the mesonic potential:

$$M_1^2 = \frac{1}{2} \left[2U_{\vec{\pi}^2} + 4\vec{\pi}^2 U_{\vec{\pi}^2\vec{\pi}^2} + U_{\sigma\sigma} + \sqrt{(2U_{\vec{\pi}^2} + 4\vec{\pi}^2 U_{\vec{\pi}^2\vec{\pi}^2} - U_{\sigma\sigma})^2 + 16\vec{\pi}^2 U_{\sigma\vec{\pi}^2}^2} \right], \\ M_2^2 = 2U_{\vec{\pi}^2}, \quad M_3^2 = 2U_{\vec{\pi}^2}, \\ M_4^2 = \frac{1}{2} \left[2U_{\vec{\pi}^2} + 4\vec{\pi}^2 U_{\vec{\pi}^2\vec{\pi}^2} + U_{\sigma\sigma} - \sqrt{(2U_{\vec{\pi}^2} + 4\vec{\pi}^2 U_{\vec{\pi}^2\vec{\pi}^2} - U_{\sigma\sigma})^2 + 16\vec{\pi}^2 U_{\sigma\vec{\pi}^2}^2} \right]. \quad (7)$$

For $\vec{\pi}^2 = 0$, the masses of the three pion modes are degenerate. The symmetry breaking terms in the σ -direction do not affect the $O(3)$ -symmetry of the pion subspace, so that the pion fields appear only in the combination $\vec{\pi}^2$ in the eigenvalues. The constituent quark mass is given by

$$M_q^2 = g^2[(\sigma + m_c)^2 + \vec{\pi}^2] \quad (8)$$

To derive renormalization group flow equations in a finite four-dimensional volume $L^3 \times T$, we replace the integrals over the momenta in the evaluation of the trace (3) by a sum

$$\int dp_i \dots \rightarrow \frac{2\pi}{L} \sum_{n_i=-\infty}^{\infty} \dots \quad (9)$$

We are free in the choice of boundary conditions for the bosons and fermions in the space directions. However, in the time direction, the boundary conditions are fixed by the statistics of the fields. Adopting the language of lattice literature, we use T to denote the length of the finite volume box in Euclidean time direction. Then the Matsubara frequencies take the values

$$\omega_{n_0} = \frac{2\pi n_0}{T} \quad \text{and} \quad \nu_{n_0} = \frac{(2n_0 + 1)\pi}{T}. \quad (10)$$

for bosons and for fermions, respectively. In the following we use the short-hand notation

$$p_p^2 = \frac{4\pi^2}{L^2} \sum_{i=1}^3 n_i^2 \quad \text{and} \quad p_{ap}^2 = \frac{4\pi^2}{L^2} \sum_{i=1}^3 \left(n_i + \frac{1}{2} \right)^2 \quad (11)$$

for the three-momenta in the case of periodic (p) and anti-periodic (ap) boundary conditions. The flow equation corresponding to eq. (5) is

$$k \frac{\partial}{\partial k} U_k(\sigma, \vec{\pi}^2, T, L) = \frac{k^{2(a+1)}}{TL^3} \sum_{n_0} \sum_{\vec{n}} \left(- \frac{4N_c N_f}{(k^2 + \nu_{n_0}^2 + p_{ap,p}^2 + M_q^2(\sigma, \vec{\pi}^2))^{a+1}} \right. \\ \left. \sum_{i=1}^{N_f^2=4} \frac{1}{(k^2 + \omega_{n_0}^2 + p_p^2 + M_i^2(\sigma, \vec{\pi}^2))^{a+1}} \right). \quad (12)$$

The sums in eq. (12) run from $-\infty$ to $+\infty$, where the vector \vec{n} denotes (n_1, n_2, n_3) . For both finite and infinite volume, we choose $a = 2$ for the cutoff function. For a volume with infinite extent in time direction $T \rightarrow \infty$, we perform the sum over the Matsubara frequencies analytically [19]:

$$k \frac{\partial}{\partial k} U_k(\sigma, \vec{\pi}^2, T \rightarrow \infty, L) = \frac{3}{16} \frac{k^6}{L^3} \sum_{\vec{n}} \left(- \frac{4N_c N_f}{(k^2 + p_{ap,p}^2 + M_q^2(\sigma, \vec{\pi}^2))^{5/2}} \right. \\ \left. \sum_{i=1}^{N_f^2=4} \frac{1}{(k^2 + p_p^2 + M_i^2(\sigma, \vec{\pi}^2))^{5/2}} \right) \quad (13)$$

Note that we employ both flow equations (12) and (13) for our numerical calculations in the next section. We would like to make one comment: The insertion of the regulator function (4) in the Schwinger proper-time integral is not necessary to regularize the infrared regime, since finite volume calculations are already infrared finite. However, if we keep the volume fixed, the insertion of the regulator function is needed to integrate out the quantum fluctuations in a controlled way.

In order to solve the partial differential equations (5) and (12), we project these flow equations on the following ansatz for the mesonic potential [15]:

$$U_k(\sigma, \vec{\pi}^2) = \sum_{i=0}^{N_\sigma} \sum_{j=0}^{i+j \leq N_\sigma} a_{ij}(k) (\sigma - \sigma_0(k))^i (\sigma^2 + \vec{\pi}^2 - \sigma_0(k)^2)^j. \quad (14)$$

Performing such a projection, we get, in principle, an infinite set of coupled first-order differential equations. To solve this set of equations, we have to truncate the ansatz at some power in $(\sigma - \sigma_0(k))$ and $(\sigma^2 + \vec{\pi}^2 - \sigma_0(k)^2)$. In this paper, we use $N_\sigma = 2$. The resulting finite set of flow equations can be solved straightforwardly in a numerical calculation.

III. CALCULATION

We have solved the RG flow equations numerically and will present the results for the volume dependence of the pion mass and the pion decay constant in the following section. First we discuss some details about the numerical evaluation and the determination of the coefficients of the ansatz for the potential eq. (14) at the UV scale. At the ultraviolet cutoff scale Λ_{UV} , the meson potential can be characterized by the values of the couplings m_{UV} and λ_{UV} in eq. (2). All other coefficients in the ansatz eq. (14) are set to zero. In order to solve the flow equations for the effective potential, we truncate the ansatz for the potential as discussed in the last section. In the present work, we expand the potential up to mass dimension four in the mesonic fields. Furthermore, we have to specify a value for the current quark mass m_c , which controls the degree of explicit symmetry breaking. The Yukawa coupling g does not evolve in the present approximation [16, 17, 20]. We choose $g = 3.26$, which leads to a reasonable constituent quark mass of $M_q = g(f_\pi + m_c) \approx 310$ MeV for physical values for the pion decay constant $f_\pi = 93$ MeV and the current quark mass $gm_c = 7$ MeV.

In table I, we summarize the three parameter sets which we use in obtaining our results for pion masses of 100, 200 and 300 MeV, see also ref. [15]. In our comparison of different boundary conditions, we use the same parameter sets to obtain results for either periodic or anti-periodic boundary conditions for the fermions. We determine these UV parameters by fitting to the pion mass $m_\pi(\infty)$ and to the corresponding pion decay constant $f_\pi(\infty)$, which is taken in infinite volume from chiral perturbation theory [4]. We then evolve the RG equations with these parameters to predict the volume dependence of $f_\pi(L)$ and $m_\pi(L)$.

Λ_{UV} [MeV]	m_{UV} [MeV]	λ_{UV}	gm_c [MeV]	f_π [MeV]	m_π [MeV]
1500	779.0	60	2.10	90.38	100.8
1500	747.7	60	9.85	96.91	200.1
1500	698.0	60	25.70	105.30	300.2

TABLE I: Values for the parameters at the *UV*-scale used in the numerical evaluation. We determine these parameters by fitting in infinite volume to a particular pion mass $m_\pi(\infty)$ and the corresponding value of the pion decay constant $f_\pi(\infty)$, taken from chiral perturbation theory. In our notation, the physical current quark mass corresponds to gm_c . We use $g = 3.26$.

From table I, we can read off that the pion mass is primarily determined by the value of the current quark mass, which controls the explicit symmetry breaking. To obtain the correct value for the pion decay constant for a given pion mass, the meson mass at the UV scale m_{UV} has to be decreased from 780 MeV to 700 MeV when the pion mass increases from 100 to 300 MeV. We use the same value for the four-meson-coupling λ_{UV} for all values of the pion mass and pion decay constant considered here. The possible values of the current quark mass are limited by the requirement that all masses, in particular the sigma-mass, must remain substantially smaller than the ultraviolet cutoff $\Lambda_{UV} \approx 1500$ MeV of the model. We have checked that our results are to a large degree independent of the particular choice of UV parameters: different sets of starting parameters give the same volume dependence, provided that they lead to the same values of the pion mass and pion decay constant in infinite volume.

We use the result of chiral perturbation theory for the dependence of the pion decay constant on the pion mass to facilitate the comparison between the quark meson model and chPT. However, it is possible to get the correct behavior of the pion decay constant as a function of a single symmetry breaking parameter with renormalization group methods, as was shown in infinite volume [18].

For anti-periodic boundary conditions for the fermions, we have previously investigated the dependence of our results on the cutoff scale Λ_{UV} [15] and found it to be small for light pions, and only moderate for the largest pion mass we considered here. We argued that such a trend towards a stronger cutoff dependence for larger pion masses was to be

expected, since the existence of a cutoff becomes more relevant for heavier mesons. This analysis still pertains to the results with anti-periodic boundary conditions presented here. For a choice of periodic boundary conditions, however, the cutoff dependence of the results is somewhat more pronounced, in particular for small volumes when the Euclidean time extent is kept large. Varying the cutoff between 1.5 GeV and 1.1 GeV for a pion mass of $m_\pi(\infty) = 300$ MeV, we find that the largest variations are of the order of 5 – 6% of the pion mass, and take place in a volume range of $L = 0.5 – 1.0$ fm, depending on the exact ratio T/L of time and space extent. As we argue below, this is mainly due to effects on the quark condensation: for periodic boundary conditions, a larger UV cutoff allows for the build-up of a larger condensate in finite volume, since for any given volume, a larger number of momentum modes $2\pi|\vec{n}|/L$ remain below the cutoff and contribute. In a volume region where the quarks dominate the finite volume effects, a certain cutoff dependence of these effects is therefore expected in this model.

The sums over the momentum modes in the flow equations cannot be performed analytically, therefore we have to truncate the sums at a maximal mode number $N_{max} = \max|\vec{n}|$. With this truncation, we introduce an additional UV cutoff in our calculation. In order to guarantee that this cutoff does not affect our results we require

$$\frac{2\pi}{L} N_{max} \gg \Lambda_{UV}. \quad (15)$$

We have to take care that this relation is well satisfied since we are using a "soft" cutoff function. We have checked the dependence of the results on N_{max} in [15] and found that it is sufficient to use $N_{max} = 40$ for $\Lambda_{UV} = 1.5$ GeV and volumes up to $L = 5$ fm, which we will also use for the calculations in this paper. The numerical evaluation of the sums over the momentum modes simplifies significantly if we take the box sides as integer multiples of some length scale L_0 , such that $L = n_L L_0$ and $T = n_T L_0$. Therefore we restrict ourselves to this case. Below, we show that the results for the low-energy observables strongly depend on the ratio $T/L = n_T/n_L$.

IV. RESULTS

We have calculated the pion mass shift

$$R[m_\pi(L)] = \frac{m_\pi(L) - m_\pi(\infty)}{m_\pi(\infty)} \quad (16)$$

with both choices for the fermionic boundary conditions for three different pion masses, $m_\pi(\infty) = 100, 200$ and 300 MeV, and for infinite ($T/L \rightarrow \infty$) as well as for finite extent of the Euclidean time axis with different ratios $T/L = 3/1, 3/2, 1/1$.

In Fig. 2, we show the results for the pion mass shift with periodic boundary conditions as a function of the box size L . The three panels show the results for the three different pion masses we investigated, and the curves are labeled with the ratios T/L . The main new and surprising observation is that in this case, for certain volume ranges, the mass of the pion in the finite volume can be *lower* than in infinite volume. In particular, this is the case for pion masses $m_\pi(\infty) \geq 200$ MeV, ratios $T/L \geq 3/2$, and volumes smaller than 2 fm: $R[m_\pi(L)]$ takes on negative values and develops a minimum. This can be seen in the lower two panels of Fig. 2. Secondly, we note that this minimum in the mass shift becomes deeper for larger pion masses $m_\pi(\infty)$, and the corresponding larger values of $f_\pi(\infty)$. For $m_\pi(\infty) = 300$ MeV, the pion mass shift reaches down to approximately $R[m_\pi] = -0.14$ at $L = 0.7$ fm.

In Fig. 3, we compare the results for the pion mass shift with periodic (p. b.c.) and anti-periodic (a.p. b.c.) boundary conditions for the fermion fields, for the ratios $T/L = 3/2$ and $T/L = 1/1$. Clearly, employing p. b.c. lowers the relative mass shift $R[m_\pi(L)]$, compared to using a.p. b.c.. The differences become larger in smaller volumes, for larger pion masses $m_\pi(\infty)$, and with increasing ratios T/L . As we have seen, if the length of the box in the Euclidean time direction is taken to infinity, for large pion masses the pion mass can be smaller in finite than in infinite volume, so that the finite volume shift becomes negative.

Although at first a surprising result, this shift to smaller pion masses can actually be explained in the framework of the quark-meson model and its mechanism of chiral symmetry breaking. In order to show this, we resort to a version of the model that is simplified compared to our ansatz (14), but still contains the same essential structure. In this model, for a fixed symmetry breaking parameter gm_c , the pion mass is completely specified by the scale-dependent order parameter $\sigma_0(k, L)$, and by the values given at the UV scale for the coupling g and the meson mass m_{UV}^2 . According to [21, 22], it is

$$M_\pi^2(k, L) = \frac{m_c m_{UV}^2}{\sigma_0(k, L)}. \quad (17)$$

For periodic boundary conditions, the “squeezing” of the quark fields in a small finite volume leads to an increase in the chiral quark condensate, before a further decrease of the volume size induces a restoration of chiral symmetry. Following eq. (17), the increase in the order

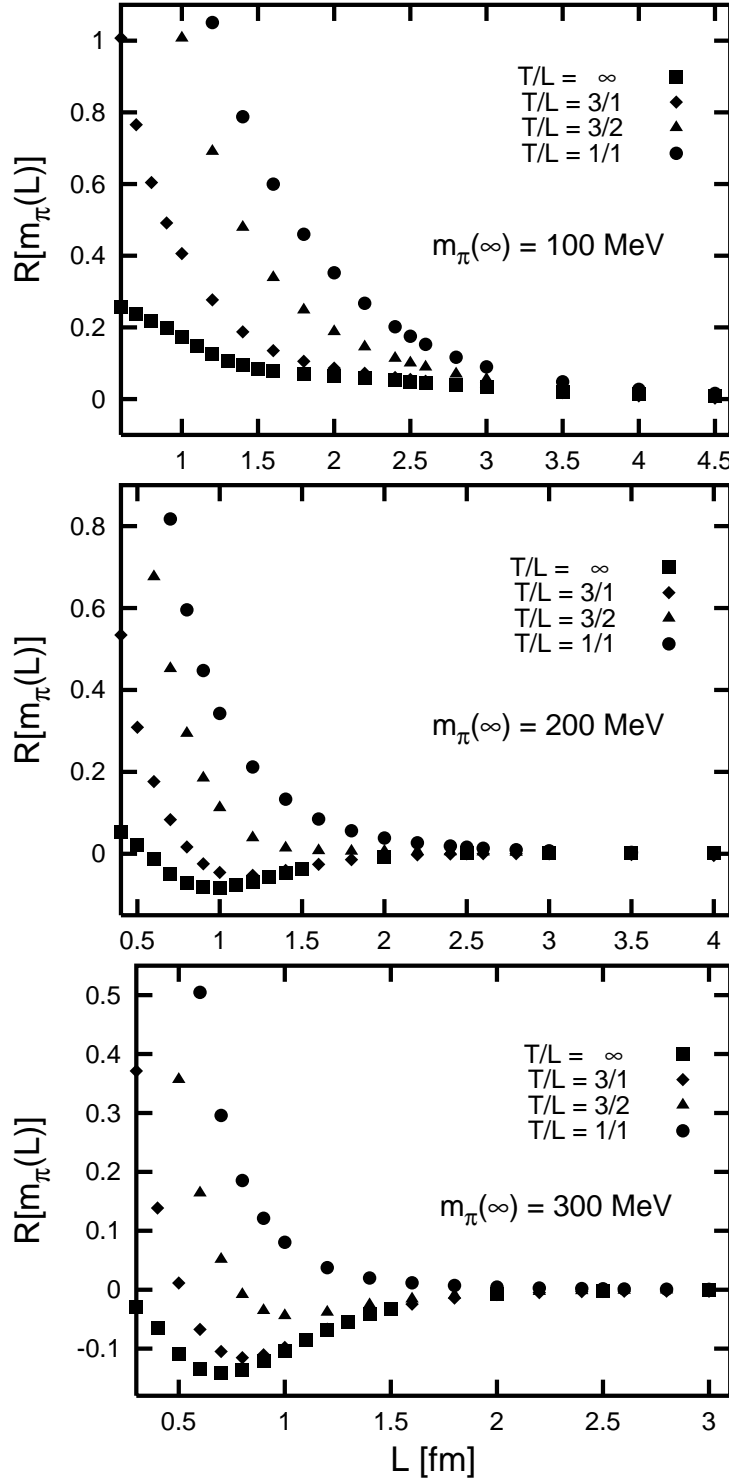


FIG. 2: Results for the pion mass shift $R[m_\pi(L)] = (m_\pi(L) - m_\pi(\infty))/m_\pi(\infty)$, in a finite Euclidean volume of size $V = L^3 \times T$, for periodic boundary conditions. The ratio of T/L for the different curves is given in the figure. We show the results for pion masses of $m_\pi(\infty) = 100, 200, 300$ MeV (identified in the figure).

parameter leads in turn to the observed decrease in the pion mass.

The intermediate increase in the order parameter with the decreasing volume size can be explained more rigorously from the flow equations. Since this increase occurs in volumes that are already quite small, the flow is dominated by the zero-momentum modes and it is sufficient to analyze the contributions of these modes.

The zero mode contribution to the flow equation from quarks and mesons is for purely periodic boundary conditions in spatial directions given by

$$\left[k \frac{\partial}{\partial k} U_k(\sigma, \vec{\pi}^2, L, T) \right]_0 = -\frac{k^{2(a+1)}}{TL^3} \left(2 \cdot \frac{4N_c N_f}{(k^2 + \nu_0^2 + M_q(k, L, \sigma, \vec{\pi}^2)^2)^{(a+1)}} \right. \\ \left. - \frac{N_f^2 - 1}{(k^2 + M_\pi(k, L, \sigma, \vec{\pi}^2)^2)^{(a+1)}} - \frac{1}{(k^2 + M_\sigma(k, L, \sigma, \vec{\pi}^2)^2)^{(a+1)}} \right) \quad (18)$$

where $\nu_0^2 = (\pm\pi/T)^2$ corresponds to the value of the two Matsubara frequencies closest to zero. The prefactor $1/L^3$ diverges for $L \rightarrow 0$ for all momentum modes, but enhances only the zero modes: For the non-zero momentum modes, the enhancement is canceled and they are in fact strongly suppressed, which is due to the factors $1/L^2$ of the momentum terms in the denominators. If we scale T proportional to L , because of the Matsubara frequencies this suppression occurs also for the lowest fermionic terms, although it is much weaker. The result of this competition between suppression and enhancement for the fermions depends on the ratio T/L .

We first consider exclusively the contributions of the fermionic zero modes, which exist only for periodic boundary conditions:

$$\left[k \frac{\partial}{\partial k} U_k(\sigma, \vec{\pi}^2, T, L) \right]_0^F = -\frac{k^{2(a+1)}}{TL^3} \cdot 2 \cdot \frac{4N_c N_f}{(k^2 + \nu_0^2 + M_q^2(\sigma, \vec{\pi}^2))^{a+1}} \quad (19)$$

This truncation to the fermionic contributions only is equivalent to the leading term of a large N_c -approximation, as it is shown in [23]. In principle, eq. (19) can be integrated analytically, since the constituent quark mass, given by $M_q^2(\sigma, \vec{\pi}^2) = g^2[(\sigma + m_c)^2 + \vec{\pi}^2]$, does not depend on any scale-dependent quantities. The result shows that the zero mode contributions to the potential as a function of the expectation value are *repulsive* for small values. Consequently, these contributions increase the expectation value $\sigma_0(k, L)$ and thus the value of the pion decay constant. Since these zero-momentum contributions are enhanced for small volumes, this explains the increase in the expectation value.

Alternatively, this can be understood in more detail by a direct analysis of the zero mode contributions to the flow equation for the minimum $\sigma_0(k, L)$ of the potential. Since the flow

equation for $\sigma_0(k, L)$ is obtained from the minimum condition

$$\frac{\partial}{\partial \sigma} U_k(\sigma = \sigma_0(k, L), \vec{\pi}^2 = 0, L, T) = 0, \quad (20)$$

it is determined by the flow of the potential. As we have seen in our analysis above, the fermionic contributions tend to increase the absolute value of the minimum $\sigma_0(k, L)$, while the mesonic contributions tend to decrease it. Thus, we can perform this analysis entirely by considering the zero mode part of the potential flow given in eq. (18).

The renormalization scale k controls the momenta of the quantum fluctuations that are integrated out. As soon as this momentum scale drops below the mass of one of the degrees of freedom, that particular field can no longer contribute to the RG evolution of the running couplings: it decouples from the RG flow. We restrict the discussion here to scales $k < m_\sigma$, where the sigma meson has already decoupled.

With periodic boundary conditions, the finite box length in the Euclidean time direction T is the only scale which affects the zero modes. The scale π/T is in competition with the renormalization scale k , and if k drops below this scale, the lowest Matsubara frequency $\nu_0 = \pi/T$ acts as a cutoff and stops that part of the evolution which is driven by the quark fields. If T is sufficiently small, this happens already above the scale at which chiral symmetry breaking sets in. In that case, condensation of the quark fields is prevented, and the constituent quark mass remains small. This means that $m_\pi(k \rightarrow 0, L)$ remains large and that $R[m_\pi(L)]$ is large and positive. This is illustrated by the results for $T/L = 1/1$ and small L in Fig. 2.

The situation is different for large values of $T/L > 3/2$. Here, the additional scale set by $1/T$ plays a less important role and becomes relevant only for much smaller volumes. In this case, quarks build up a large condensate. According to eq. (17), this increase in the chiral condensate leads to a decrease of the pion mass, which is visible in Fig. 2 for $T/L > 3/2$, $m_\pi(\infty) \geq 200$ MeV, and $L \geq 0.8$ fm. For large values of T/L , the decrease in the condensate for small volumes cannot be explained by the presence of the cutoff π/T for the quark fields alone. There is an additional mechanism that decreases σ_0 in such a way that chiral symmetry is broken less strongly. For very small volumes, the pion contributions in eq. (18) dominate the flow of σ_0 . Even for a large ratio T/L , this leads to a decrease in σ_0 and the observed rise in $R[m_\pi(L)]$ for small L .

For anti-periodic boundary conditions, we do not find any decrease of $R[m_\pi(L)]$ with

decreasing finite volume size L for any value of T/L , as can be seen in the comparison in Fig. 3. As we have argued in [15], in our RG approach with anti-periodic boundary conditions, two effects are responsible for the finite volume behavior: effects due to the quark condensation, and effects due to light pions which appear after the chiral condensate has been built up by the quark fields. In contrast to the case of periodic boundary conditions, for anti-periodic boundary conditions the formation of the quark condensate is strongly suppressed by the lowest possible momentum for the fermions, which is $\sqrt{3}\pi/L$, see eq. (11), and acts as an infrared cutoff. Consequently, for small L , fewer modes contribute to the chiral condensate. If in addition T/L is small, the condensate decreases further and we observe a larger mass shift $R[m_\pi(L)]$.

Finally, in Fig. 4 we compare our results for the pion mass shift to the results of chiral perturbation theory. (Note that Fig. 4 has a logarithmic scale, whereas Figs. 2 and 3 have linear scales.) We present results for different pion masses from RG calculations with both periodic and anti-periodic boundary conditions for the fermions, and from chiral perturbation theory [4, 6]. For the chPT results, the pion mass shift is calculated with the help of Lüscher's formula [24], which relates the leading corrections of the pion mass in finite Euclidean volume to the $\pi\pi$ -scattering amplitude in infinite volume. The sub-leading corrections drop as $\mathcal{O}(e^{-\bar{m}L})$ with $\bar{m} \geq \sqrt{3/2}m_\pi$. Using a calculation of the $\pi\pi$ -scattering amplitude in chPT to three loops (*nnlo*) as input for Lüscher's formula, the authors of ref. [4] obtain a correction above the leading order, which is then added to the one-loop result of Gasser and Leutwyler [25]. Lüscher's original approach only considers the periodicity of pion propagators in finite volume as an invariance under a shift by L . More recently, in ref. [6] this has been improved to account for the fact that these propagators are actually invariant under shifts by $\vec{n}L$ with arbitrary \vec{n} . The result is a Lüscher formula resummed over \vec{n} , which is very similar to the original one. The finite volume shift for the pion mass is significantly increased by this resummation. In [15] we have carefully compared our RG results with anti-periodic boundary conditions to the chPT results from [4]. Here, we use the improved results from [6] for the comparison. The RG results are still consistently above the results from chPT. Lüscher's approach becomes an increasingly better approximation with increasing pion mass for a given volume size. The decreasing differences between the chPT results and the RG results with increasing pion mass are compatible with this estimate. For large volumes, the mass shift is completely controlled by pion effects and drops as $e^{-m_\pi L}$,

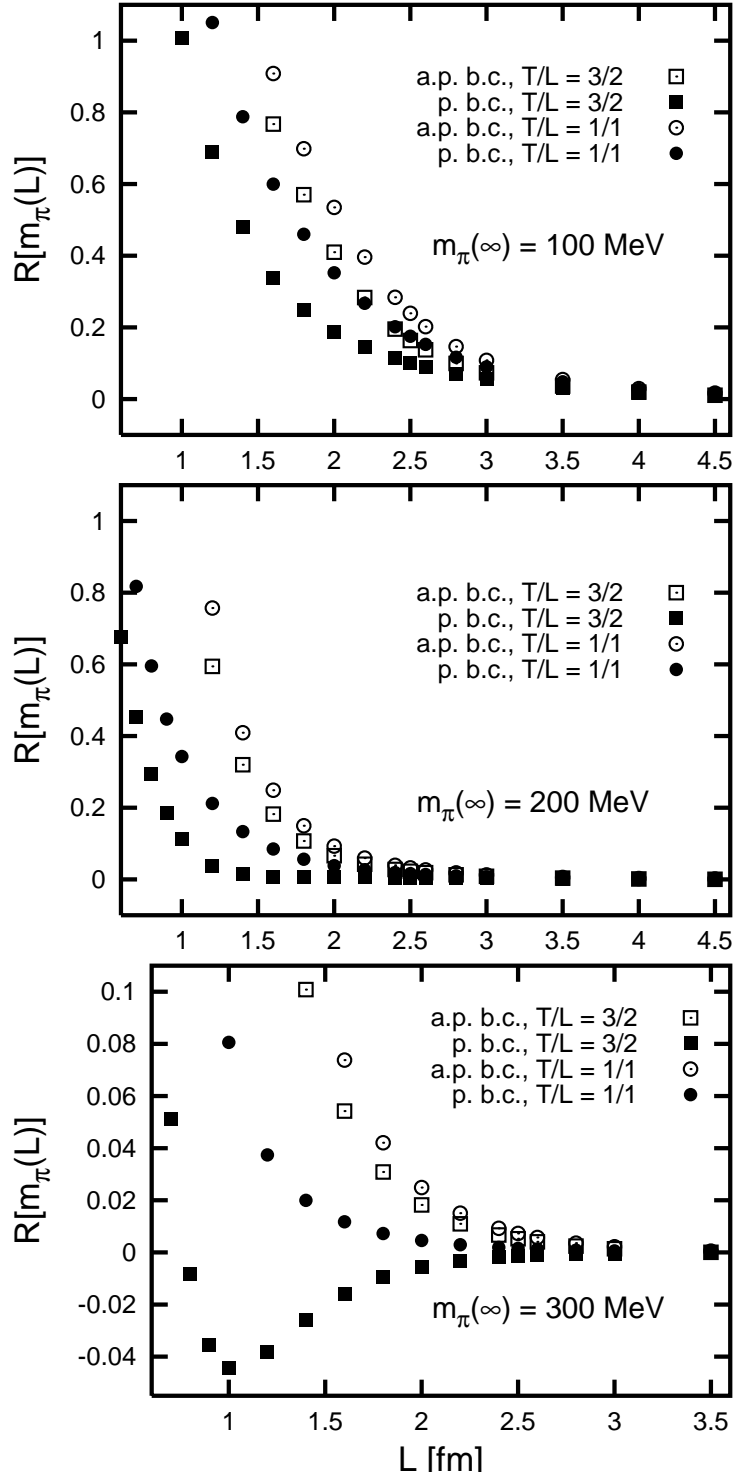


FIG. 3: Comparison of the pion mass shift in finite volume $R[m_\pi(L)] = (m_\pi(L) - m_\pi(\infty))/m_\pi(\infty)$ for the two choices of fermionic boundary conditions. Open symbols denote results for anti-periodic, solid symbols for periodic boundary condition. The size of the volume is $V = L^3 \times T$, the ratios of T/L for the different curves are given in the figures. We show results for pion masses of $m_\pi(\infty) = 100, 200, 300$ MeV (identified in the figure).

so that both the RG and the chPT results have the same slope in the logarithmic plot. For the entire volume range shown in Fig. 4, the RG and chPT results apparently differ only by a factor which is almost independent of the volume size. For $m_\pi(\infty) = 300$ MeV, the chPT and RG results agree within errors. For small volumes, however, the RG approach has the advantage that it can be extended to describe the transition into a regime with approximately restored chiral symmetry, where the chiral expansion becomes unreliable.

The mesonic degrees of freedom are less affected by the ratio T/L . The upper curve in Fig. 4 represents RG calculations with anti-periodic boundary conditions and $T/L = 1/1$, which gives a larger $R[m_\pi(L)]$ compared to the lower curve corresponding to $T/L = \infty$. Fluctuations due to the light pions yield a decrease of the condensate and explain the increase of $R[m_\pi(L)]$ for larger volumes. In particular for small pion masses ($m_\pi = 100$ MeV) and the ratio $T/L = 1/1$, the results with periodic and with anti-periodic boundary conditions overlap over a wide volume range. From our analysis, for sufficiently small values of $m_\pi(\infty)$ this is expected in the region where pion dynamics dominate. Because of this, the slopes of the curves are very similar. The deviations between results at the same, fixed ratio T/L that differ only in the choice of boundary conditions become larger for increasing pion masses $m_\pi(\infty)$ and decay constants $f_\pi(\infty)$. This indicates that fermionic effects are increasingly important. Evidence for this is also the observation that the results for the pion mass shift with periodic boundary conditions have a smaller slope, compared to the results with anti-periodic boundary conditions, and also compared to those of chPT. The reason is that the cutoff scales are different: for periodic boundary conditions, the lowest fermion momentum mode is given by the lowest Matsubara frequency $\nu_0 = \pi/T$, and not determined by $\sqrt{3}\pi/L$ as for anti-periodic boundary conditions. In particular for large values of T/L , this explains that the finite volume mass shift will be much larger for anti-periodic boundary conditions. For small volumes, we thus find the importance of quark effects confirmed by the dependence on the boundary conditions. But since pion effects dominate for larger volumes, the results of chPT and of our RG approach converge for large L .

V. COMPARISON TO LATTICE RESULTS AND CONCLUSIONS

The main motivation for our current investigation is the possible application to lattice gauge theory, as already stated in the introduction. At present, lattice calculations can only

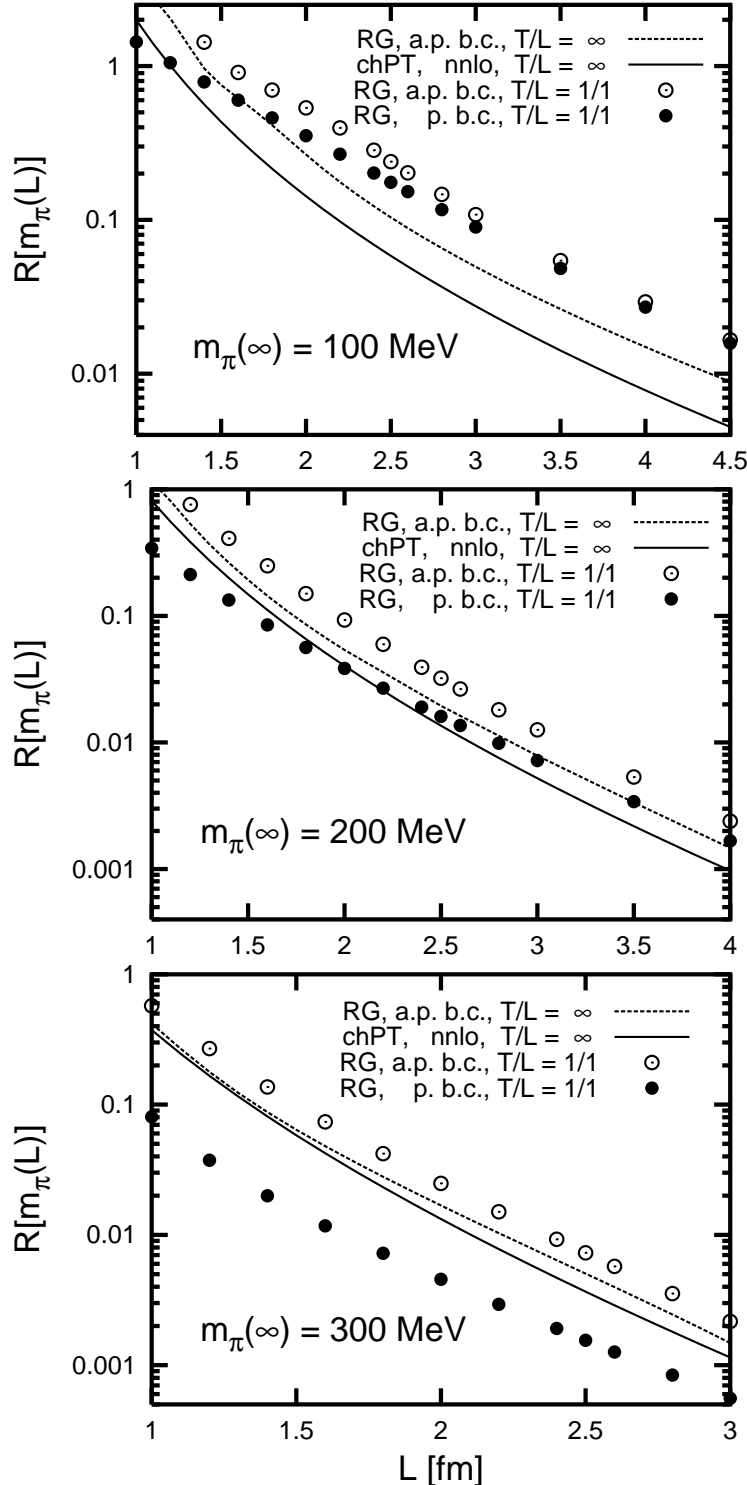


FIG. 4: Comparison of the pion mass shift $R[m_\pi(L)] = (m_\pi(L) - m_\pi(\infty))/m_\pi(\infty)$ for different boundary conditions with the results of chiral perturbation theory [6] on a logarithmic scale. The ratio of T/L for the different curves is given in the figures. We show results for a pion mass of $m_\pi(\infty) = 100, 200, 300$ MeV (identified in the figure).

be performed on relatively small lattices of the order of at most $2 - 3$ fm, and for large pion masses of $500 - 700$ MeV. The more accurate these calculations are, the more important it becomes to understand finite size effects and to control the finite size extrapolation.

Our model incorporates chiral symmetry and can still be used in the vicinity of the point where chiral symmetry is restored. Finite volume effects should therefore be captured as far as they relate to chiral symmetry breaking. But it is not a gauge theory, there are no gluons, and consequently the constituent quarks in this model are not confined. There is no guarantee that the same mechanisms apply as in QCD.

Extrapolations to infinite volume using chiral perturbation theory are extremely successful in the description of the volume dependence of nucleon properties, such as for example the nucleon mass [3, 7]. However, as far as meson masses are concerned, the finite volume mass shifts observed on the lattice deviate from the predictions of chiral perturbation theory. This holds also [10] for Lüscher's approach [24], which only takes pion effects into account as well. Generally, the predicted mass shifts are much smaller than the observed ones [10, 11, 12, 13]. The inclusion of higher orders in the chiral expansion [4] and a summation of additional contributions in Lüscher's expression [6] increase the size of the predicted mass shifts and decrease the distance to the RG results.

The issue of finite volume effects has been addressed in several lattice studies [10, 11, 12, 13, 26]. The pion mass shift $R[m_\pi(L)]$ calculated by the ZeRo collaboration [11], which is shown in Fig. 1, actually becomes negative and has a minimum at small volume sizes. Although this negative shift is small, the result seems to be significant. The minimum is most pronounced for small quark masses (at $\kappa = 0.1350$). The position of the minimum corresponds to $m_\pi L = 3.5$ or $L = 1.264$ fm with $T/L = 2.25$. The results were obtained in the quenched approximation with periodic boundary conditions for the quark fields. Similar observations have also been made in [10, 12], where the simulations were performed with dynamical Wilson quarks.

In our calculation, such a decrease in the pion mass is reproduced if we choose periodic boundary conditions for the quarks. The minimum appears for large pion mass $m_\pi(\infty) = 300$ MeV, $T/L \geq 3/2$ and $L = 1$ fm, cf. Fig. 2. Our model suggests a mechanism for the appearance of this minimum, which may be the same mechanism as on the lattice. In contrast to our findings, however, the decrease of the pion mass in finite volume seems to be larger for smaller infinite-volume pion mass. For lattice calculations, several other

mechanisms for finite volume mass shifts have been suggested, from an interaction of hadrons with their mirror states on a periodic lattice [26] to effects on quark propagation related to a breaking of the center symmetry of the gauge group [13].

The influence of boundary conditions for sea and valence quarks in lattice simulations was also studied by Aoki *et al.* [13]. They find that periodic boundary conditions lead to a lower mass shift than anti-periodic boundary conditions (see table III of [13]). This finding is in agreement with our results, as can be seen in Figs. 3 and 4. The actual pion mass on the lattice is very high (> 1 GeV). Different choices for the boundary conditions of sea and valence quarks make it possible for the authors to establish a connection between the mass shift and the expectation value that Polyakov loops acquire in the presence of sea quarks. They relate the large increase of the pion mass observed for small lattice size to the restoration of chiral symmetry. This is illustrated by their results for the chiral condensate (Fig. 10 of [13]), which decreases strongly in small volumes. In the same figure, the condensate may increase for intermediate volume size, which would be similar to the behavior of the order parameter seen in our simple model. We agree that the mass shift in small volumes is due to chiral symmetry restoration, and reproduce this result in our calculations.

Comparing our results to those from chiral perturbation theory, we find agreement only for large volumes and larger pion masses, provided we impose anti-periodic boundary conditions on the fermionic fields. As expected, the differences increase for very small volumes, where chiral symmetry restoration becomes important. For periodic boundary conditions, large pion masses, and a large ratio T/L , the mass shifts in small volumes behave differently from those of chPT. Our results reproduce the qualitative behavior of the lattice results.

Our RG approach improves our understanding of the mechanisms of finite volume effects in QCD, but cannot yet give a model independent extrapolation formula to relate finite lattice results to the hadronic world.

In conclusion, we have discussed effects of quark boundary conditions on the finite volume shifts of the pion mass. We used the framework of an RG treatment of the quark-meson model to offer a possible mechanism which accounts for quark effects. Our approach shows the importance of the fermionic boundary conditions for the pion mass and the pion decay constant. The differences between the results for periodic and anti-periodic boundary conditions increase for increasing pion mass and increasing ratio T/L . Our analysis agrees

qualitatively with the observations from lattice QCD, in regards to the dependence on quark boundary conditions as well as in regards to an apparent drop of the pion mass in finite volume. We find convergence of our results to those of chiral perturbation theory calculations for large pion masses and large volumes, where quark effects are not important.

Acknowledgments

The authors would like to thank G. Colangelo for providing the data for the comparison to chPT in Fig. 4. B.K. would like to thank I. Wetzorke and K. Jansen for a useful discussion. J.B. would like thank the GSI for financial support.

[1] M. Procura, T. R. Hemmert, and W. Weise, Phys. Rev. **D69**, 034505 (2004), hep-lat/0309020.

[2] D. Arndt and C. J. D. Lin, Phys. Rev. **D70**, 014503 (2004), hep-lat/0403012.

[3] A. Ali Khan et al. (QCDSF-UKQCD), Nucl. Phys. **B689**, 175 (2004), hep-lat/0312030.

[4] G. Colangelo and S. Dürr, Eur. Phys. J. **C33**, 543 (2004), hep-lat/0311023.

[5] G. Colangelo and C. Haefeli, Phys. Lett. **B590**, 258 (2004), hep-lat/0403025.

[6] G. Colangelo, S. Dürr, and C. Haefeli (2005), hep-lat/0503014.

[7] P. F. Bedaque, H. W. Griesshammer, and G. Rupak (2004), hep-lat/0407009.

[8] D. B. Leinweber, D. H. Lu, and A. W. Thomas, Phys. Rev. **D60**, 034014 (1999), hep-lat/9810005.

[9] W. Detmold, W. Melnitchouk, J. W. Negele, D. B. Renner, and A. W. Thomas, Phys. Rev. Lett. **87**, 172001 (2001), hep-lat/0103006.

[10] S. Aoki et al. (JLQCD), Phys. Rev. **D68**, 054502 (2003), hep-lat/0212039.

[11] M. Guagnelli et al. (Zeuthen-Rome (ZeRo)), Phys. Lett. **B597**, 216 (2004), hep-lat/0403009.

[12] B. Orth, T. Lippert, and K. Schilling (2005), hep-lat/0503016.

[13] S. Aoki et al., Phys. Rev. **D50**, 486 (1994).

[14] S. Aoki et al., Nucl. Phys. Proc. Suppl. **34**, 363 (1994), hep-lat/9311049.

[15] J. Braun, B. Klein, and H. J. Pirner, Phys. Rev. **D71**, 014032 (2005), hep-ph/0408116.

[16] D. U. Jungnickel and C. Wetterich, Phys. Rev. **D53**, 5142 (1996), hep-ph/9505267.

[17] B.-J. Schaefer and H.-J. Pirner, Nucl. Phys. **A660**, 439 (1999), nucl-th/9903003.

- [18] D. U. Jungnickel and C. Wetterich, Eur. Phys. J. **C2**, 557 (1998), hep-ph/9704345.
- [19] J. Braun, K. Schwenzer, and H.-J. Pirner, Phys. Rev. **D70**, 085016 (2004), hep-ph/0312277.
- [20] J. Berges, D. U. Jungnickel, and C. Wetterich, Phys. Rev. **D59**, 034010 (1999), hep-ph/9705474.
- [21] J. D. Walecka, Oxford Stud. Nucl. Phys. **16**, 1 (1995).
- [22] J. Zinn-Justin, Int. Ser. Monogr. Phys. **113**, 1 (2002).
- [23] J. Meyer, K. Schwenzer, H.-J. Pirner, and A. Deandrea, Phys. Lett. **B526**, 79 (2002), hep-ph/0110279.
- [24] M. Lüscher, Commun. Math. Phys. **104**, 177 (1986).
- [25] J. Gasser and H. Leutwyler, Phys. Lett. **B188**, 477 (1987).
- [26] M. Fukugita, H. Mino, M. Okawa, G. Parisi, and A. Ukawa, Nucl. Phys. Proc. Suppl. **30**, 365 (1993).